Slit2 Prevents Neutrophil Recruitment and Renal Ischemia-Reperfusion Injury

Swasti Chaturvedi,*[†‡] Darren A. Yuen,*[‡§||] Amandeep Bajwa,[¶] Yi-Wei Huang,[‡] Christiane Sokollik,[‡] Liping Huang,[¶] Grace Y. Lam,[†‡] Soumitra Tole,[†] Guang-Ying Liu,[‡] Jerry Pan,[‡] Lauren Chan,[‡] Yaro Sokolskyy,[‡] Manoj Puthia,[**] Gabriela Godaly,[**] Rohan John,[††] Changsen Wang,[||] Warren L. Lee,[†||] John H. Brumell,[†‡‡‡] Mark D. Okusa,[¶] and Lisa A. Robinson*[†‡]

*Division of Nephrology, Hospital for Sick Children, Toronto, Ontario, Canada; [†]Institute of Medical Science and [‡‡]Department of Molecular Genetics, University of Toronto, Ontario, Canada; [‡]Program in Cell Biology, Hospital for Sick Children Research Institute, Hospital for Sick Children, Toronto, Ontario, Canada; [§]Division of Nephrology, St. Michael's Hospital, Toronto, Ontario, Canada; [||]Keenan Research Centre, Li Ka Shing Knowledge Institute, St. Michael's Hospital, Toronto, Ontario, Canada; [¶]Department of Medicine and Center for Immunity, Inflammation and Regenerative Medicine, University of Virginia, Charlottesville, Virginia; [**]Institute of Laboratory Medicine, Section of Microbiology, Immunology and Glycobiology, Lund University, Lund, Sweden; and [††]Department of Laboratory Medicine and Pathobiology, University Health Network, Toronto, Ontario, Canada

ABSTRACT

Neutrophils recruited to the postischemic kidney contribute to the pathogenesis of ischemia-reperfusion injury (IRI), which is the most common cause of renal failure among hospitalized patients. The Slit family of secreted proteins inhibits chemotaxis of leukocytes by preventing activation of Rho-family GTPases, suggesting that members of this family might modulate the recruitment of neutrophils and the resulting IRI. Here, in static and microfluidic shear assays, Slit2 inhibited multiple steps required for the infiltration of neutrophils into tissue. Specifically, Slit2 blocked the capture and firm adhesion of human neutrophils to inflamed vascular endothelial barriers as well as their subsequent transmigration. To examine whether these observations were relevant to renal IRI, we administered Slit2 to mice before bilateral clamping of the renal pedicles. Assessed at 18 hours after reperfusion, Slit2 significantly inhibited renal tubular necrosis, neutrophil and macrophage infiltration, and rise in plasma creatinine. In vitro, Slit2 did not impair the protective functions of neutrophils, including phagocytosis and superoxide production, and did not inhibit neutrophils from killing the extracellular pathogen *Staphylococcus aureus*. In vivo, administration of Slit2 did not attenuate neutrophil recruitment or bacterial clearance in mice with ascending *Escherichia coli* urinary tract infections and did not increase the bacterial load in the livers of mice infected with the intracellular pathogen *Listeria monocytogenes*. Collectively, these results suggest that Slit2 may hold promise as a strategy to combat renal IRI without compromising the protective innate immune response.

AKI develops in 5% of hospitalized patients and leads to significant morbidity, mortality, and financial costs.[1–3] Fifty percent of AKI cases result from ischemia-reperfusion injury (IRI).[4] Despite significant advances in the understanding of kidney IRI pathogenesis, specific therapy remains elusive, and management is mainly supportive.[5]

IRI leads to the recruitment of circulating leukocytes, particularly neutrophils, into the injured kidney.[6–9] After recruited, neutrophils

exacerbate damage by releasing inflammatory mediators.[10–12] Therapies targeting only single aspects of neutrophil recruitment are only partially effective in ameliorating renal injury.[13,14] Given the diversity of neutrophil attractants and the involvement of other leukocyte subsets, it is unlikely that a single antichemotactic therapy will be entirely effective.[15] A generalized strategy to inhibit recruitment of inflammatory leukocytes would be more beneficial.

The Slit family of secreted proteins and their receptor Roundabout (Robo) repel neurons during central nervous system development.[16,17] Slit has three known isoforms (Slit1–3), and Robo has four isoforms (Robo-1 to -4).[18] The persistent expression of Slit and Robo in the mature organism suggests biologic functions that extend beyond development.[19] We and others have previously shown that Slit2 and Robo-1 inhibit chemotaxis of neutrophils, T lymphocytes, and dendritic cells to diverse chemoattractants.[20–23] The role of Slit2 in modulating renal inflammation associated with AKI, however, has not been previously explored.

Here, we report that Slit2 potently inhibits multiple steps involved in recruitment of circulating neutrophils. *In vivo*, we show that Slit2 administration prevents tubular injury, neutrophil infiltration, and renal failure associated with postischemic AKI. We also show that Slit2 does not impair critical protective immune functions of neutrophils and does not increase susceptibility to bacterial infection. These results suggest that Slit2 represents a potential strategy for the prevention and treatment of AKI without compromising protective host innate immune functions.

RESULTS

Endogenous Levels of Slit2 Decrease in the Kidney after IRI

To explore the role of Slit2 in IRI, we first examined endogenous renal Slit2 levels in a mouse model of bilateral kidney IRI that mimics clinical ischemic AKI.[24–26] Although Slit2 protein was detected in the glomeruli and tubulointerstitium of sham-operated kidneys, a significant downregulation of Slit2 levels was noted after ischemia-reperfusion (Figure 1).

Slit2 Inhibits Neutrophil Adhesion to Activated Endothelial Cells

We showed that neutrophils express the Slit2 receptor, Robo-1 (Supplemental Figure 1), and that Slit2 inhibits neutrophil chemotaxis to diverse chemoattractants by preventing activation of Rho-family guanosine triphosphatases (GTPases).[22] The reduction in renal Slit2 after IRI suggested its potential involvement in regulating neutrophil recruitment. Because multiple steps in neutrophil recruitment are Rho-family GTPase-dependent, we established cell culture models to examine the effects of Slit2 on each step of neutrophil recruitment in the setting of IRI. We first tested the effects of Slit2 on
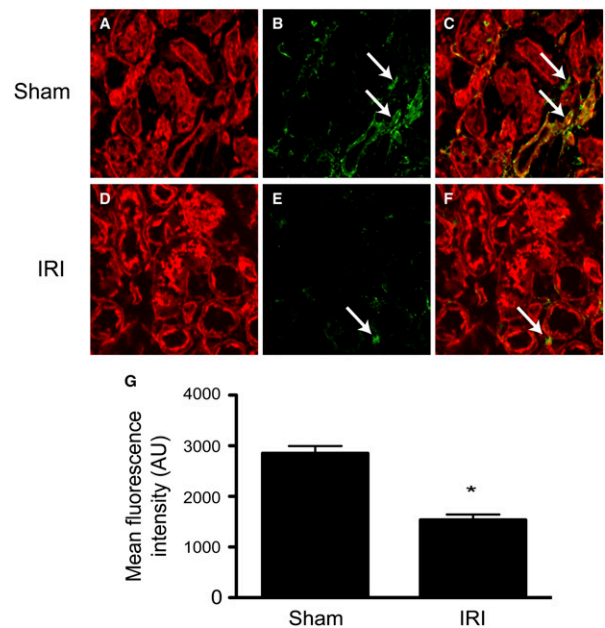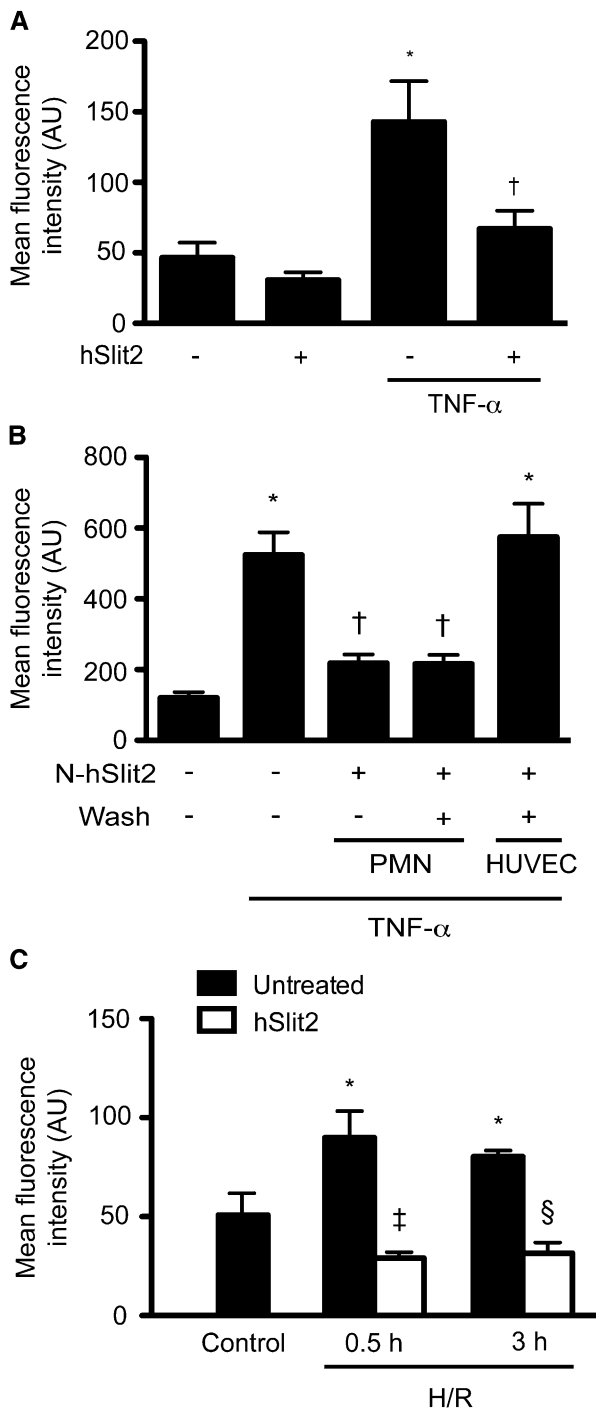

Figure 1. Slit2 protein levels decrease in the kidney after IRI. Representative images of frozen kidney sections immunofluorescently labeled with anti-Slit2 antibody and Alexa 488 anti-goat IgG (green) from mice subjected to (A–C) sham surgery and (D–F) IRI. Original magnification, ×20. (A and D) DiI-conjugated wheat germ agglutinin staining (red) was performed to delineate cell membranes. (B and E) Immunolabeled Slit2 (green) and (C and F) merged images. White arrows indicate interstitial Slit2 staining. (G) Quantitative analysis of Slit2 levels using Volocity software was performed on 10 random, nonoverlapping 20× cortical fields sampled from sham surgery (n=3) and IRI kidneys (n=6) immunofluorescently labeled for Slit2. Data are presented as mean ± SEM. *P<0.05 versus sham surgery kidneys.

adhesion of human neutrophils to human umbilical vein endothelial cells (HUVEC) stimulated by TNF-α, an inflammatory cytokine locally upregulated after IRI.[27] Although neutrophils only minimally adhered to unstimulated HUVEC, their adhesion was enhanced after TNF-α activation of HUVEC (Figure 2A, P<0.05 versus control). In the presence of full-length human Slit2 (hSlit2), neutrophil adhesion decreased (Figure 2A, P<0.05 versus TNF-α–stimulated HUVEC).

To confirm the specificity of this inhibition, we used a bioactive N-terminal fragment of hSlit2 (N-hSlit2). N-hSlit2 inhibited neutrophil adhesion to endothelium activated by TNF-α (Figure 2B and Supplemental Figure 2, P<0.05 versus TNF-α–stimulated HUVEC). We also used a soluble truncated species of the Robo-1 receptor (RoboN), which acts as a decoy receptor for Slit2.[28] Preincubation of N-hSlit2 with RoboN abrogated the effects of N-hSlit2 (Supplemental Figure 2), indicating that the inhibitory effects of Slit2 are Robo-1–dependent.

The observed effects of Slit2 on neutrophil adhesion could result from direct actions on neutrophils and/or HUVEC. HUVEC expressed Robo-1, -2, and -4, suggesting that these

cells may also be Slit2-responsive (Supplemental Figure 3).[29] To determine whether the observed effects of Slit2 result from its actions on neutrophils and/or endothelial cells, neutrophils were first incubated with N-hSlit2, after which unbound N-hSlit2 was washed away before performing the adhesion assays. When unbound Slit2 was removed, neutrophil adhesion was inhibited to the same extent as when Slit2 was present throughout the assay (Figure 2B). Conversely, when HUVEC were incubated with Slit2 and unbound Slit2 was then removed, neutrophil adhesion was not inhibited (Figure 2B). Collectively, these data show that Slit2 acts directly on neutrophils and not endothelial cells to impair neutrophil adhesion to injured endothelium.

Slit2 Inhibits Neutrophil Adhesion to Endothelial Cells Subjected to Hypoxic Injury

Although TNF-α is an important endothelial activator that is upregulated after IRI, it is only one of a number of such signals. We, therefore, examined the effect of Slit2 on neutrophil adhesion to endothelial cells exposed to hypoxia-reoxygenation (H/R), confirming first that H/R resulted in endothelial injury (Supplemental Figure 4).[30] When HUVEC were exposed to 2 hours of hypoxia followed by 0.5 or 3 hours of reoxygenation, neutrophil adhesion increased (Figure 2C, $P<0.05$ versus control). Neutrophils preincubated with hSlit2 adhered less to HUVECs exposed to H/R after reoxygenation periods of both 0.5 and 3 hours (Figure 2C, $P<0.05$ hSlit2-treated versus untreated neutrophils).

Slit2 Reduces Neutrophil Capture by and Adhesion to Activated Endothelial Cells

The static adhesion assays described above test the effects of Slit2 on neutrophil adhesion in the absence of shear flow. To test steps upstream of firm neutrophil adhesion in a system more closely representative of the *in vivo* setting, we used a microfluidic system to examine neutrophil–endothelial interactions under shear flow conditions that mimic the renal microvasculature.[31] Although only 8±1 neutrophils interacted with endothelium per high power field (hpf) under basal conditions after 1 minute of flow (Supplemental Video 1), the

Figure 2. Slit2 inhibits neutrophil adhesion to activated endothelial cells. Freshly isolated human neutrophils were labeled with calcein and incubated with PBS, full-length hSlit2, or the bioactive N-hSlit2. Neutrophils (10^5 cells/well) were incubated with confluent HUVEC monolayers and allowed to adhere for 30 minutes. Nonadherent cells were removed, and neutrophil adhesion was quantified using a fluorescent plate reader at excitation and emission wavelengths of 494 and 517 nm, respectively. (A) The effects of hSlit2 on neutrophil adhesion to HUVEC prestimulated with TNF-α. (B) To determine whether the observed effects of Slit2 result from its actions on neutrophils and/or endothelial cells, neutrophils were incubated with N-hSlit2 for 10 minutes, and unbound N-hSlit2 was washed away before performing the adhesion assays. In parallel experiments, endothelial cells were incubated with N-hSlit2, and unbound N-hSlit2 was washed away before performing the adhesion assays. (C) Hypoxic conditions were induced by exposing HUVEC to 1% oxygen at 37°C. Cells were exposed to 2 hours of hypoxia followed by the indicated periods of reoxygenation, and neutrophil adhesion assays were performed as in A. *$P<0.05$ versus basal. †$P<0.05$ versus TNF-α stimulation. ‡$P<0.05$ versus HUVEC exposed to 2 hours of hypoxia followed by 0.5 hours of reoxygenation. §$P<0.05$ versus HUVECs exposed to 2 hours of hypoxia followed by 3 hours of reoxygenation. Mean values ± SEM from three to five independent experiments.

number of interacting neutrophils increased after HUVEC stimulation with TNF-α to 53±4 cells/hpf (Figure 3A and Supplemental Video 2, $P<0.01$ versus basal). In the presence of hSlit2, the number of rolling and adherent neutrophils interacting with activated endothelium was reduced (Figure 3A and Supplemental Video 3, $P<0.05$ TNF-α versus TNF-α + hSlit2). When Slit2 was preincubated with RoboN, its inhibitory effect was attenuated (Supplemental Figure 5 and

Supplemental Video 4). Collectively, these data show that, under shear flow, Slit2 prevents the initial capture and adhesion of neutrophils to activated endothelium.

These early effects also translated into a significant reduction in total neutrophil adhesion at later time points. After 12 minutes of shear flow, under basal conditions, there was minimal neutrophil adhesion to endothelium. Although activation of HUVEC with TNF-α increased neutrophil adhesion ($P<0.05$ versus basal), this adhesion was reduced by preincubating the neutrophils with Slit2 (Figure 3, B and C, $P<0.05$ versus TNF-α).
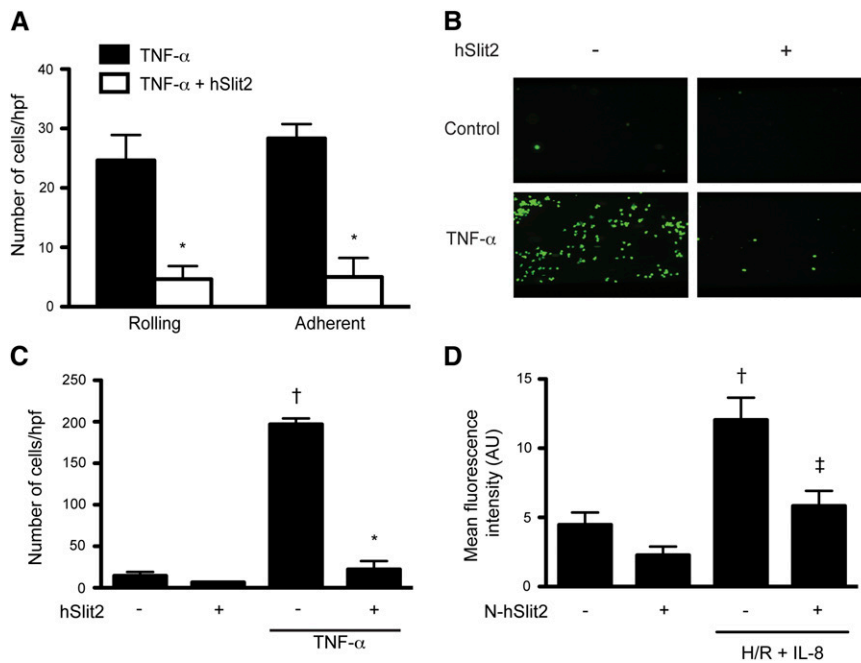
Figure 3. Slit2 inhibits neutrophil capture by, adhesion to, and transendothelial migration across activated endothelial cells under shear flow conditions. HUVEC grown to confluence in channels of the Bioflux microfluidic system were incubated with TNF-α for 4 hours. Calcein-labeled human neutrophils were preincubated with PBS or hSlit2 and then perfused through the channels at a shear rate of 0.5 dynes/cm². A Nikon TE2000 inverted microscope and Hamamatsu video camera were used to video record neutrophil–HUVEC interactions. Neutrophil adhesion was quantified using Bioflux Montage software. (A) Neutrophil–endothelial interactions were recorded after 1 minute of flow at 0.5 dynes/cm², and the number of neutrophils that were rolling and firmly arrested was determined. (B) Neutrophil adhesion to the endothelial monolayer was determined after 12 minutes of shear flow at 0.5 dynes/cm², and representative images were taken from three to five independent experiments using a 20× objective. (C) Experiments were performed as in B, and the number of neutrophils was quantified. (D) To assess the effects of Slit2 on neutrophil transendothelial migration, HUVEC were grown to confluence on fibronectin-coated polyester transwell inserts placed in a 24-well plate and exposed to hypoxia (2 hours) followed by reoxygenation (0.5 hours). Calcein-labeled human neutrophils were incubated with PBS or Slit2 (4.5 μg/ ml) for 10 minutes and placed in the upper well of the transwell chamber, and the chemokine IL-8 (50 ng/ml) was added to the lower well. Neutrophils were allowed to migrate for 3 hours at 37°C. Neutrophils that had migrated from the upper to the lower well were permeabilized with 1% Triton, and the fluorescence emitted was read using a fluorescent plate reader. Mean values ± SEM from three independent experiments. *$P<0.05$ versus TNF-α–stimulated HUVECs. †$P<0.05$ versus basal HUVEC. ‡$P<0.05$ versus IL-8 treatment and HUVEC exposure to 2 hours of hypoxia followed by 0.5 hours of reoxygenation.

Slit2 Reduces Chemoattractant-Induced Neutrophil Transendothelial Migration

After neutrophils firmly adhere to the injured endothelium, they undergo Rho-family GTPase-dependent transmigration across the endothelial barrier to infiltrate the injured kidney in response to the local release of chemoattractants, such as IL-8.[32–34] We tested the effect of Slit2 on IL-8–mediated transendothelial migration of neutrophils in the absence or presence of H/R injury. Although IL-8 increased neutrophil migration across uninjured or H/R-injured HUVEC monolayers (Figure 3D and Supplemental Figure 6, $P<0.05$ versus control), hSlit2 decreased neutrophil transendothelial migration to near basal values (Figure 3D and Supplemental Figure 6, $P<0.05$ versus IL-8).

Slit2 Prevents Renal IRI

Having shown that Slit2 inhibits multiple steps in neutrophil recruitment, we next examined the effect of Slit2 administration on mice subjected to renal IRI. After 18 hours, plasma creatinine was more than sevenfold higher in mice that underwent bilateral renal IRI compared with sham-treated mice (Figure 4A, $P<0.05$). hSlit2 administration prevented the rise in plasma creatinine in a dose-dependent manner (Figure 4A, vehicle versus Slit2 at 1 μg, $P<0.05$; vehicle versus Slit2 at 2 μg, $P<0.05$; Slit2 at 2 μg versus Slit2 at 1 μg, $P<0.05$). Administration of a bioactive N-terminal fragment of mouse Slit2 (N-mSlit2) also reduced plasma creatinine (Figure 4B, $P<0.05$), whereas preincubation of N-mSlit2 with RoboN attenuated this protective effect (Figure 4B).

The change in renal function was associated with parallel changes in morphology
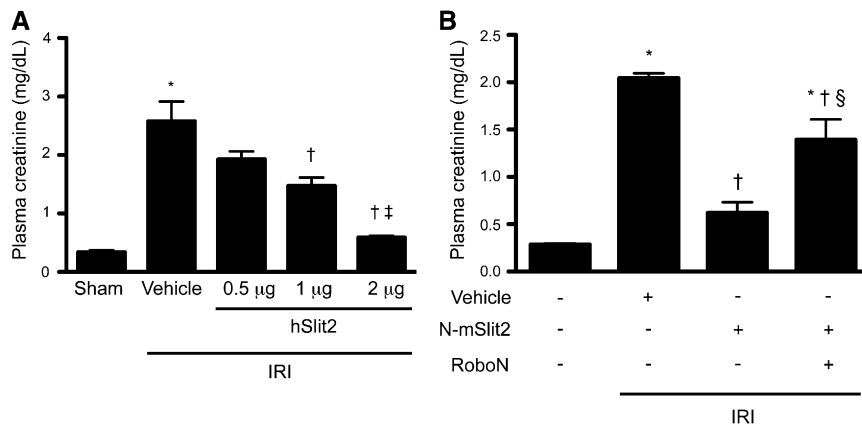
Figure 4. Slit2 prevents renal dysfunction after IRI. (A) IRI was induced by bilateral cross-clamping of renal pedicles of male C57BL/6 mice for 26 minutes. Full-length hSlit2 (at the indicated doses) or vehicle was administered intraperitoneally before inducing IRI; 18 hours after reperfusion, blood was drawn by retro-orbital bleed, and plasma creatinine was determined using a colorimetric assay. (B) Truncated N-mSlit2 (2 μg) with or without molar equivalent amounts of RoboN was administered intraperitoneally before induction of renal IRI, and experiments were performed as in A. Mean values $\pm$ SEM from four to seven mice per experimental group. *$P<0.05$ versus sham-operated mice. †$P<0.05$ versus vehicle-treated IRI mice. ‡$P<0.05$ versus hSlit2 1 μg-treated IRI mice. §$P<0.05$ versus N-mSlit2–treated IRI mice.

(Figure 5, A–D). After IRI, there was a marked increase in tubular injury compared with sham mice (Figure 5, A, B, and E, $P<0.05$). Both hSlit2 and N-mSlit2 administration reduced this injury (Figure 5, C and E, $P<0.05$ N-mSlit2 versus vehicle, and Supplemental Figure 7, $P<0.05$ hSlit2 versus vehicle). In contrast, blockade of N-mSlit2 with RoboN before administration to IRI mice attenuated the tubuloprotective effects of Slit2 (Figure 5, D and E, $P<0.05$).

IRI also led to an increase in renal neutrophil infiltration compared with sham-operated controls (Figure 5F, $P<0.05$). N-mSlit2 treatment reduced renal neutrophil numbers ($P<0.05$ versus vehicle), whereas preincubation of N-mSlit2 with RoboN abrogated this effect (Figure 5F, $P<0.05$). Preadministration of hSlit2 also reduced renal neutrophil and macrophage infiltration (Supplemental Figure 8, $P<0.05$ versus vehicle). Collectively, these data show that Slit2 administration reduces IRI-induced renal dysfunction, structural injury, and neutrophil infiltration into the injured kidney.

Slit2 Does Not Inhibit Neutrophil Phagocytosis, Superoxide Production, or Bacterial Killing *In Vitro*

Because renal IRI is often associated with critical illness, where infection is a common occurrence, we questioned whether exogenous Slit2 might inhibit protective neutrophil immune functions, such as phagocytosis of opsonized particles and superoxide production.[35] Using a latex bead phagocytosis assay, we found that Slit2 did not affect neutrophil phagocytosis, with 77.7%$\pm$7.1% of untreated neutrophils and 80.6%$\pm$7.0% of Slit2-treated neutrophils ingesting at least one opsonized bead (untreated versus Slit2-treated mean phagocytic index: 3.5$\pm$0.6 versus 3.7$\pm$0.4).

Using an assay of superoxide production, we next tested whether Slit2 inhibits the respiratory burst after neutrophil activation.[22] Although unstimulated neutrophils did not produce detectable superoxide (data not shown), formyl-methionyl-leucyl-phenylalanine (fMLP) treatment enhanced neutrophil superoxide production to 20.6$\pm$0.6 nmol/10^7 cells per minute. Preincubation of neutrophils with Slit2 did not impair superoxide production but rather, promoted a modest increase (27.8$\pm$1.2 nmol/10^7 cells per minute, $P<0.05$).

We next tested the effects of Slit2 on neutrophil killing of the extracellular pathogen *Staphylococcus aureus*, a common cause of bacterial sepsis in critically ill patients with renal IRI. After bacteria were incubated with neutrophils for 90 minutes, the bacterial colony count in the untreated neutrophil sample decreased to 61%$\pm$13% of the starting count, whereas the bacterial count in the Slit2-treated neutrophil samples displayed an even greater reduction (Figure 6A, $P<0.05$). Thus, Slit2 did not impair neutrophil killing of *S. aureus* but rather, enhanced it.

Slit2 Treatment Does Not Impair Immune Protection against Bacterial Infection *In Vivo*

To further explore the effect of Slit2 on innate immunity, we tested its actions in two established models of infection. First, Slit2 was administered to mice inoculated with the intracellular pathogen *Listeria monocytogenes*. At all times ranging from 0.5 to 48 hours, hepatic bacterial counts, reflective of neutrophil activity, were similar between vehicle- and Slit2-treated mice (Figure 6B), indicating that Slit2 administration does not impair protective innate immune responses against intracellular pathogens.[36]

We also tested the effects of administering Slit2 on clearance of uropathogenic *Escherichia coli* in a murine model of ascending urinary tract infection.[37,38] Because neutrophils are essential for antibacterial defense of the genitourinary tract, we assessed the effects of Slit2 on neutrophil recruitment and bacterial clearance.[39,40] Neutrophil numbers in the urine and bacterial colony counts in the urine and kidney were similar between vehicle- and Slit2-treated mice (Figure 7). Taken together, these results suggest that Slit2 administration does not impair immune protection against bacterial infections *in vivo*.

DISCUSSION

AKI continues to exact high rates of morbidity and mortality in hospitalized patients,[41] with IRI being the leading cause of AKI
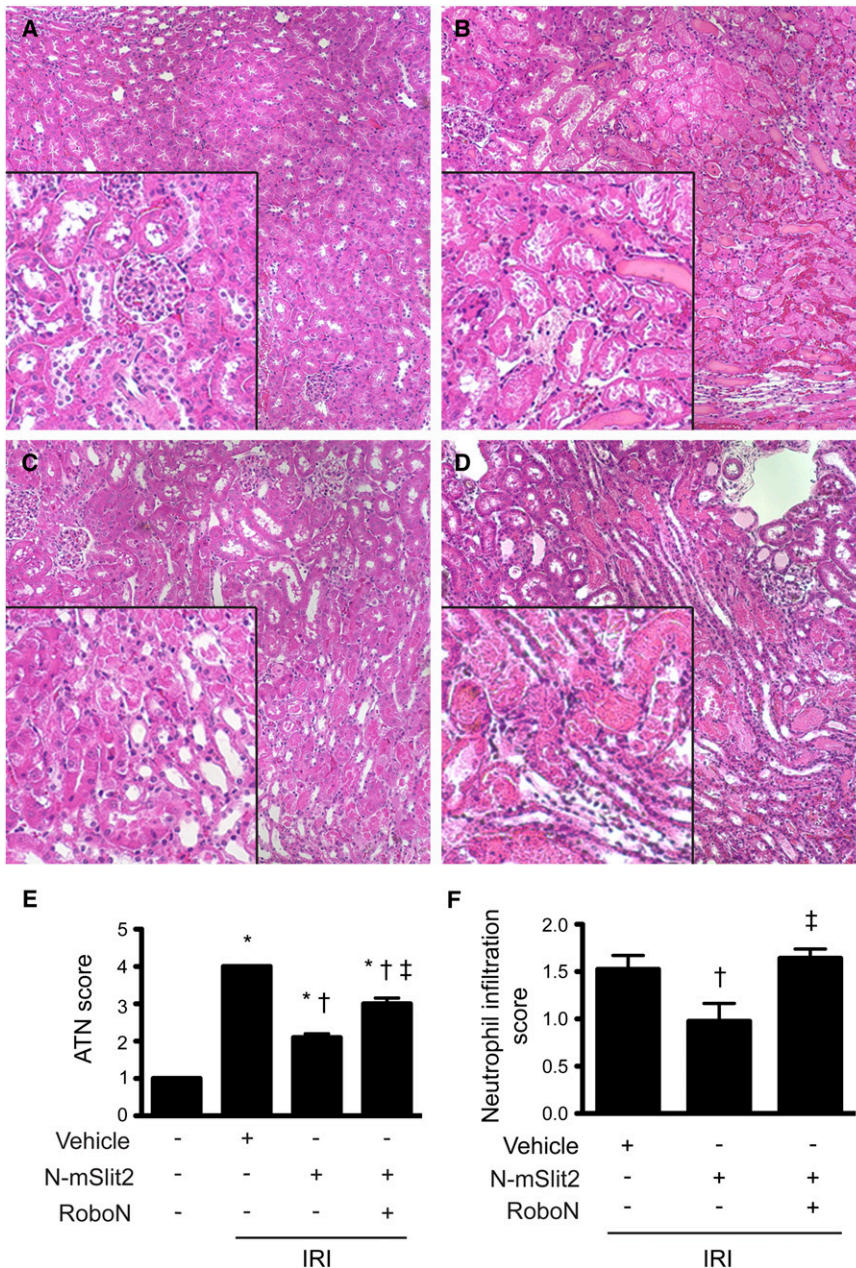
Figure 5. Slit2 improves acute tubular necrosis and reduces neutrophil infiltration after renal IRI. (A–D) Representative hematoxylin and eosin-stained kidney sections from mice subjected to (A) sham surgery, (B) vehicle administration before IRI, (C) N-mSlit2 administration before IRI, and (D) N-mSlit2–RoboN administration before IRI examined using a Zeiss AxioSkop microscope equipped with a SPOT-RT Camera. Original magnification, ×20; ×2 in insets. (E) To quantify the degree of tubular injury, kidney sections were examined using a Zeiss AxioSkop microscope and scored by counting the percentage of tubules that displayed cell necrosis, loss of brush border, cast formation, and tubular dilation; they were scored as follows: 1<10%, 2=10%–25%, 3=26%–50%, 4=51%–75%, and 5>75%. Two to three fields from the outer medulla of each section were evaluated. Original magnification, ×200. (F) Experiments were performed as in Figure 4, and kidneys were collected after 18 hours. Kidneys were weighed, minced, and digested with collagenase type IA (10 μg/ml). The cell pellet was washed, nonspecific Fc binding was blocked with anti-mouse CD16/32 antibody (2.4G2), and cell suspensions were incubated with fluorophore-tagged anti-mouse CD45 antibody (30-F11) to determine total leukocyte cell numbers. Anti-CD45 antibody-labeled samples were further labeled with anti-mouse GR-1-FITC antibody (Ly6G) and anti-mouse CD11b-PE antibody to identify neutrophils. Appropriate fluorochrome-conjugated, isotype-matched, irrelevant monoclonal antibodies were used as negative controls. Flow cytometry data acquisition was performed on BD FACS Calibur, and data were analyzed using FlowJo software 6.4. The number of GR-1$^+$CD11b$^+$CD45$^+$ neutrophils was normalized to kidney weight, indexed to the value for sham surgery kidneys, and log-transformed to generate a neutrophil infiltration score. Mean values ± SEM from experiments involving four to seven mice per experimental group. ATN, acute tubular necrosis. *$P<0.05$ versus sham-operated mice. †$P<0.05$ versus vehicle-treated IRI mice. ‡$P<0.05$ versus N-mSlit2–treated IRI mice.

in both native and transplanted kidneys.[42,43] After IRI, the injured kidney synthesizes proinflammatory cytokines and chemokines, most notably TNF-α and IL-8, that promote renal neutrophil infiltration, a process important for IRI pathogenesis.[11,44,45] Therapies that block a specific aspect of neutrophil recruitment, such as neutrophil–endothelial adhesion, are only partially protective in mouse models of AKI.[13,14,46,47] We report that Slit2 may represent a potent strategy to inhibit multiple steps in the pathologic neutrophil recruitment seen in AKI, thus attenuating renal injury and dysfunction.

The Slit family of secreted glycoproteins was originally described in *Drosophila* as a group of neuronal repellents during central nervous system development.[16,17,48] We and others have previously shown that the Slit2 receptor, Robo-1, is also detected on leukocyte subsets, including neutrophils, T lymphocytes, monocytes, and dendritic cells.[21–23] Similar to its effects on directional axonal growth, Slit2 also inhibits leukocyte chemotactic migration.[20–22]

Here, we show that Slit2 affects not only chemotaxis of neutrophils but also, other key steps in neutrophil recruitment, such as capture, adhesion, and transendothelial migration. All of these processes, including initial neutrophil capture, involve actin cytoskeletal rearrangements, which in turn, are regulated by Rho-family GTPases, including RhoA, Cdc42, and Rac.[32,49–58] Through binding to Robo receptors, Slit2 can regulate the activity of Rho-family GTPases. Indeed,

we previously showed that, in neutrophils, Slit2 signals through Robo-1 to inhibit chemoattractant-induced polarization and activation of Rac2 and Cdc42.[22] Similarly, Slit2 inhibited chemoattractant-induced Rac activation and chemotaxis in Jurkat T cells.[21] Our work is, thus, in keeping with the work of others showing that inhibition of Cdc42 or loss of Rac activity impairs leukocyte migration across the endothelial barrier.[32,54–56] More broadly, these data suggest that Slit2 may act as a master negative switch of leukocyte recruitment processes through inhibition of Rho-family GTPases.

We hypothesized that systemic Slit2 administration would attenuate kidney IRI through binding to Robo-1 on circulating neutrophils, rendering them less responsive to local recruitment signals from the IRI kidney. Using a murine model of renal IRI, we showed that Slit2 administration significantly attenuated the rise in plasma creatinine, tubular injury, and renal neutrophil infiltration observed in mice after IRI. Similar to our findings, prior studies showed that Slit2 administration can ameliorate renal inflammation associated with crescentic GN[59] and suppress contact hypersensitivity responses.[20] Collectively, these observations show the potent anti-inflammatory properties of Slit2 in certain settings and suggest its potential as a novel therapy to prevent inflammation of diverse etiologies.

Although neutrophils are an important contributor to renal IRI pathogenesis, they also play a critical role in maintaining protective immunity against pathogens. In this regard, we found that, although Slit2 impairs chemoattractant-induced neutrophil migration,[22] it does not have a deleterious effect on protective innate immune neutrophil functions, such as phagocytosis or superoxide production. Our findings are in accordance with a previous study showing that Slit2 does not impair superoxide production by HL-60 neutrophil-like cells.[23] The varying effects of Slit2 on different neutrophil functions may be potentially explained by the complex and not fully understood roles that Rho-family GTPases play in the regulation of these processes.[60–63] Indeed, although polarization and activation of Rac and Cdc42 are known to control directional neutrophil migration,[64] their involvement in the regulation of phagocytosis is more complex. Whereas Rac1-deficient neutrophils show intact Fc (fragment, crystallizable)-mediated phagocytosis and NADPH oxidase activity, Rac2-deficient neutrophils display markedly diminished NADPH oxidase activity and phagocytosis.[60–62] In contrast, loss of Cdc42 results in normal phagocytosis and increased superoxide production.[63] In line with this report, we found that Slit2 enhanced killing of *S. aureus*, and Slit2 treatment of *L. monocytogenes*-infected mice did not increase hepatic bacterial load; both of these processes are superoxide-dependent.[65–68] In this context, our results suggest that Slit2 may selectively target polarization-dependent amplification responses within neutrophils, although the precise mechanisms through which this process may occur remain to be elucidated.

Recruitment of neutrophils to sites of injury is a complex process tightly regulated by a balance of attractant and repellent signals. After IRI, we showed that, coincident with a large neutrophil influx, endogenous levels of Slit2 in the mouse kidney are significantly reduced. Furthermore, systemic administration of exogenous Slit2 blocked neutrophil recruitment to the IRI kidney. In contrast, Slit2 treatment of mice with an *E. coli*-ascending urinary tract infection did not affect neutrophil recruitment or clearance of bacteria from the urine or kidney. These results point to the context-specific effects of Slit2 on neutrophil recruitment. Indeed, because IRI and bacterial infection can activate different sets and magnitudes of attractant and/or repellent signals, it is possible that the Slit2 responsiveness of neutrophils might vary depending on the specific balance of signals that they receive. Although beyond the scope of this study, the precise determinants of the neutrophil response to Slit2 deserve additional exploration. Nevertheless, our observation that Slit2 does not impair neutrophil antibacterial defenses points to its potential clinical use to prevent IRI without causing unwanted immunosuppression.

Neutrophils are an important mediator of renal IRI, but other cells, including macrophages, dendritic cells, and platelets, also contribute to IRI pathogenesis.[8,11] Thus, although Slit2 inhibits neutrophil recruitment in renal IRI, it may also act on other cell subsets implicated in AKI. We recently showed that Slit2 is a potent antiplatelet agent *in vitro* and *in vivo*.[69] Because activated platelets cause microvascular thrombosis in IRI, it is possible that Slit2 administration attenuated renal injury, in part, through its antiplatelet effects.[70–74] However, because platelet inhibition only partially ameliorates AKI,[75] the antiplatelet effects of Slit2 do not fully explain our results. Similarly, although Slit2 administration also reduced macrophage infiltration into the IRI kidney (Supplemental Figure 8B), agents targeting macrophages alone only partially attenuate renal injury.[76] Thus, despite the dominant role of neutrophils in the pathogenesis of renal IRI, the antineutrophil effects of Slit2 may be only one of several renoprotective activities of this pleiotropic molecule.[44,45,77]

AKI resulting from IRI remains a complex and challenging clinical problem. We report that Slit2 reduces neutrophil capture, adhesion, and transendothelial migration *in vitro* and prevents neutrophil infiltration, tubular injury, and renal failure after IRI *in vivo*. We also show that Slit2 does not impair protective neutrophil immune functions or enhance susceptibility to bacterial infection. These properties position Slit2 as an ideal therapeutic candidate for the prevention and treatment of renal IRI.

CONCISE METHODS

Chemicals and Reagents
Unless otherwise stated, reagents were purchased from Sigma-Aldrich (St. Louis, MO). Polymorphprep neutrophil separation medium was from Axis-Shield (Norway). Transwell inserts were from Corning Costar. Except as noted, all antibodies were from eBioscience (San Diego, CA) and used at a concentration of 5 μg/ml.

Slit2 Expression and Purification

Production of full-length hSlit2 and myc antibody-affinity purification were performed as previously described.[22] Bioactive truncated N-mSlit2 and N-hSlit2 were purchased from R&D systems (Minneapolis, MN) and Peprotech (Rocky Hill, NJ), respectively.

Isolation of Primary Human Neutrophils

Human whole blood was obtained from healthy volunteers, and neutrophils were isolated using Polymorphprep gradient separation as previously described.[22] Before use, neutrophils were resuspended

in HBSS containing 1 mM $CaCl_2$ and 1 mM $MgCl_2$. Experiments were performed within 1–2 hours of isolating neutrophils.[22]

Immunofluorescent Labeling of Neutrophils

Human neutrophils were seeded on fibronectin-coated coverslips and immunofluorescently labeled as previously described.[22] Cells were fixed in 4% paraformaldehyde, permeabilized, and incubated with rabbit anti-human Robo-1 antibody followed by Alexa 594-conjugated anti-rabbit IgG together with 4',6-diamidino-2-phenylindole. Cells were visualized with a spinning disc DMIRE2 confocal microscope (Leica Microsystems, Toronto, Canada) equipped with a Hamamatsu back-thinned electron microscopy charge-coupled device camera.[22]

Neutrophil–Endothelial Adhesion Assays

Neutrophil–endothelial adhesion assays were performed with minor modifications as previously described.[78–80] Freshly isolated human neutrophils were labeled with calcein and incubated with medium alone or Slit2 (4.5 μg/ml) for 10 minutes.[22] In some experiments, Slit2 was premixed with molar equivalent amounts of RoboN for 10 minutes at 37°C before incubating with neutrophils. Neutrophils (10^5 cells/well) were incubated with confluent HUVEC monolayers and allowed to adhere for 30 minutes.[81] Nonadherent cells were removed by centrifuging the 96-well plates upside down at $100 \times g$ for 1 minute. Neutrophil adhesion was quantified using a fluorescent plate reader at excitation and emission wavelengths of 494 and 517 nm, respectively. In some wells, HUVEC were incubated with TNF-α for 4 hours before
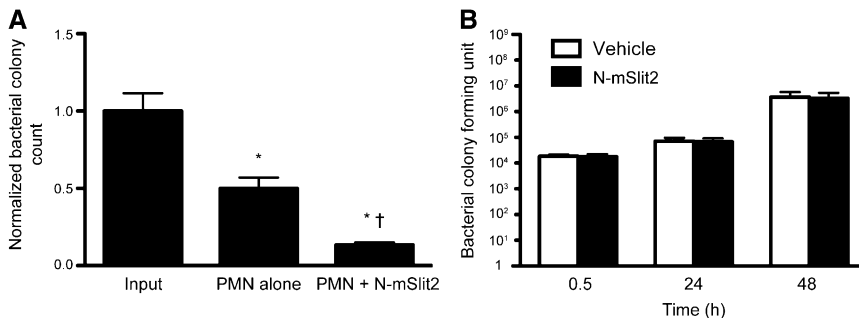
Figure 6. Slit2 does not inhibit neutrophil killing of the extracellular pathogen *S. aureus* or increase hepatic bacterial load after infection with the intracellular pathogen *L. monocytogenes*. (A) Human neutrophils (1.5×10^6) were incubated with N-mSlit2 or control vehicle at 37°C for 10 minutes, and then, 10% human serum and *S. aureus* (methicillin-resistant *S. aureus* strain CMRSA-10/USA300 at 1×10^6 CFU) were added. Samples were incubated at 37°C with 200 rpm shaking for 90 minutes. The number of viable bacteria in these suspensions was determined by plating. (B) N-mSlit2 or control vehicle was administered intravenously by tail vein injection, and *L. monocytogenes* (5×10^4 CFU in 200 μl PBS) was injected intravenously 1 hour later. At the indicated time points, mice were euthanized, the left lobe of liver was homogenized in sterile PBS, and bacterial load was determined from serial dilutions on brain heart infusion-agar plates. Mean values ± SEM from six mice per experimental group. *$P<0.05$ versus input control. †$P<0.05$ versus polymorphonuclear leukocytes alone.
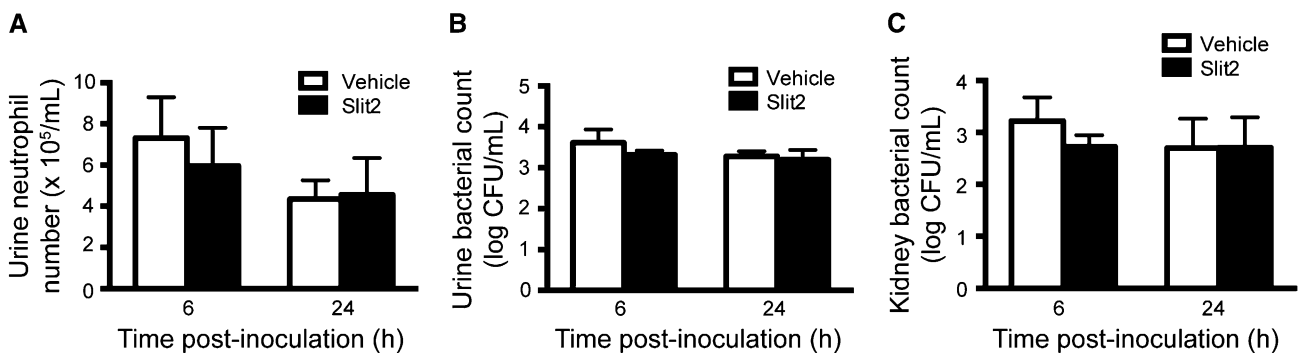
Figure 7. Slit2 does not impair neutrophil recruitment or bacterial clearance in a model of *E. coli* ascending urinary tract infection. N-mSlit2 (2 μg) or control vehicle was injected intravenously into mice 1 hour before intravesical inoculation with 10^9 CFU/ml (100 μl) uropathogenic *E. coli* CFT073 suspension; 6 and 24 hours later, urine was collected in a sterile fashion, and mice were euthanized. The kidneys were collected aseptically and homogenized, and 0.1 ml each homogenate were plated on tryptic soya agar. The number of colonies was scored after overnight culture at 37°C. (A) Urinary neutrophil concentration was calculated by hemocytometer analysis of fresh urine samples. Bacterial colony counts from (B) urine and (C) kidney homogenates are presented as log CFU per milliliter. Results were obtained from *n*=6 mice per group.

incubating with neutrophils. In parallel experiments, either neutrophils or HUVEC were incubated with Slit2 for 10 minutes, and unbound Slit2 was removed by washing before performing neutrophil–endothelial cell adhesion assays.

H/R of Endothelial Cells
To simulate IRI in an *in vitro* system, HUVEC were grown in endothelial basal medium-2 and maintained at 37°C in a standard incubator at room air oxygen tension (21% oxygen). Hypoxic conditions were induced by exposing cells to 1% oxygen and balance nitrogen at 37°C.[82] Ambient PO_2 within the chamber was calibrated and monitored during the entire experiment using a Proox 110 oxygen controller system (Biospherix). Cells were exposed to 2 hours of hypoxia followed by variable periods of reoxygenation ranging from 0.5 to 3 hours using previously described protocols.[83–86] In some wells, HUVEC were incubated with TNF-α.[87]

RT-PCR
Total RNA was isolated from HUVEC using one-step RNA reagent (BIO BASIC INC, Unionville, Canada) following the manufacturer's instructions. RT-PCR was performed using QIAGEN One-Step RT-PCR Kit (QIAGEN, Toronto, Canada) with 1 μg total RNA. The primers for human Robo-1 to -4 and corresponding RT-PCR product sizes are provided in Supplemental Table 1. Reaction mixtures were subjected to the amplification procedure as per the manufacturer's instructions. PCR products were separated by 1.5% agarose gel electrophoresis.

3-(4, 5-Dimethylthiazol-2-yl)-2,5-Diphenyltetrazolium Bromide Assays
To determine the viability of cells after H/R injury, 3-(4, 5-dimethylthiazol-2-yl)-2,5-diphenyltetrazolium bromide assays were performed as per the manufacturer's instructions.[30] Mitochondrial dehydrogenases of viable cells cleave the tetrazolium ring, yielding purple formazan crystals that are insoluble in aqueous solutions. Crystals were dissolved in acidified isopropanol, and results were read spectrophotometrically at a wavelength of 570 nm. The background absorbance was measured at 670 nm and subtracted from the 570-nm measurement. In some experiments, cells were exposed to staurosporin (1 μM) for 2 hours. All experiments were carried out in triplicate.

Microfluidic Neutrophil Adhesion Assays
To study neutrophil–endothelial interactions under shear flow, we used a microfluidics system as previously described.[69,88–93] HUVECs were grown to confluence in channels of the Bioflux microfluidic system (Fluxion Biosciences, CA) coated with fibronectin (50 μg/ml) and incubated with TNF-α for 4 hours at 37°C. Calcein-labeled human neutrophils (3×10^5/well) were preincubated with Slit2 (4.5 μg/ml) for 10 minutes and then perfused through the channels at a shear rate of 0.5 dynes/cm².[94,95] In some experiments, Slit2 (4.5 μg/ml) was premixed with molar equivalent amounts of RoboN for 10 minutes at 37°C before incubating with neutrophils. The plates were placed on the heated stage of a Nikon TE2000 inverted microscope and visualized using a 20× objective. Sequential images were recorded every 6 seconds

for up to 12 minutes in a representative field using Volocity software (Perkin-Elmer, Woodbridge, ON, Canada) interfaced with a Hamamatsu video camera. At the end of this period, four additional fields were each recorded for 30 seconds. Neutrophil adhesion was quantified with Bioflux Montage software (Fluxion Biosciences). In other experiments, neutrophil–endothelial interactions were recorded at 1 minute after initiation of flow, and the number of rolling and arrested neutrophils was determined. Only cells that remained stationary for at least 6 seconds were defined as stably adherent.[96]

Neutrophil Transendothelial Migration Assays
Neutrophil transendothelial migration assays were performed as previously described.[97,98] HUVEC were grown to confluence on fibronectin-coated polyester transwell inserts (diameter=6.5 mm, pore size=3 μm; Corning Costar) placed in a 24-well plate. Human neutrophils (5×10^6 cells/ml) were labeled with calcein and then incubated with Slit2 (4.5 μg/ml) for 10 minutes at 37°C. Thereafter, neutrophils (5×10^5/well) were placed in the upper well of the transwell chamber, and the chemokine IL-8 (50 ng/ml) was added to the lower well.[33] Neutrophils were allowed to migrate for 3 hours at 37°C. At the end of 3 hours, the neutrophils that had migrated from the upper to the lower well were permeabilized with 1% Triton, and the resulting lysates were transferred in triplicate to a 96-well plate. The fluorescence emitted was read using a fluorescent plate reader at excitation and emission wavelengths of 494 nm and 517 nm, respectively.[33] In some experiments, HUVEC were exposed to H/R as described above.

Neutrophil Phagocytosis Assays
Neutrophil phagocytosis of opsonized particles was assessed as previously described.[99] Briefly, 3.8-μm latex beads (Bang Laboratories, Inc., IN) were coated with human IgG (1 mg/ml) for 2 hours at room temperature. Neutrophils were preincubated with anti-myc Ab affinity-purified Slit2 (0.6 μg/ml) or control medium for 10 minutes, and then, they were exposed to opsonized latex beads, rapidly centrifuged (1000 rpm for 30 seconds) to initiate phagocytosis, and plated onto fibronectin-coated coverslips. Phagocytosis was terminated after 30 minutes, and external beads were labeled on ice using Cy2-conjugated anti-human IgG. Images were recorded for at least 10 random fields using a Leica deconvolution microscope (40× objective). The number of ingested particles was analyzed by counting total beads using differential interference contrast microscopy and subtracting the number of external labeled beads. Two measures were used to assess phagocytosis: (*1*) percent of neutrophils with at least one ingested bead and (*2*) phagocytic index (number of ingested beads per number of cells).[99]

Neutrophil Superoxide Production Assays
Superoxide production was assayed by measuring the superoxide dismutase inhibitable reduction of cytochrome *c*.[99] Briefly, neutrophils (2.5×10^5 cells) were incubated with anti-myc Ab affinity-purified Slit2 (0.6 μg/ml) or control medium, suspended in PBS supplemented with divalent cations and glucose, and incubated with cytochrome *c* (75 μM) $\pm$ superoxide dismutase (60 μg/ml).

Neutrophils were then stimulated with fMLP (1 μM), and cytochrome c reduction was assayed by measuring absorbance at 550 nm using a VersaMax Microplate Reader (Molecular Devices, Sunnyvale, CA) in kinetic mode for 20 minutes and acquiring readings every 15 seconds.

Neutrophil Killing of *S. aureus*

Human neutrophils (1.5×10^6) were incubated with N-mSlit2 or vehicle control at 37°C for 10 minutes, and then, 10% human serum and *S. aureus* (methicillin-resistant *S. aureus* strain CMRSA-10/USA300; 1×10^6 CFU; a gift from Andrew Simor, Sunnybrook Health Sciences Centre, Toronto, Canada) was added.[66] Samples were incubated at 37°C with 200 rpm shaking for 90 minutes. The number of viable bacteria in these suspensions was determined by plating.[66]

Mouse Renal IRI

Kidney ischemia–reperfusion surgery was performed using male C57BL/6 mice (8–12 weeks of age; Charles River Laboratories, Wilmington, MA) as previously reported.[26,45] The core temperature of the mice was maintained between 34°C and 36°C with a heating pad, and bilateral flank incisions were made under anesthesia (ketamine, 12 mg/ml; atropine, 0.48 mg/ml; xylazine, 24 mg/ml; 200 μl mixture administered per 20 g body weight). Both renal pedicles were exposed and cross-clamped for 26 minutes. Clamps were removed, and kidneys were allowed to reperfuse for 18 hours before analysis. Ambient postoperative air temperature was maintained between 30°C and 32°C until mice had fully recovered. Sham-treated mice were subjected to similar surgery without clamping of the renal pedicles. Mice were injected intraperitoneally with full-length hSlit2 at the indicated doses, N-mSlit2 (2 μg), N-mSlit2 (2 μg) premixed with molar equivalent amounts of RoboN, or vehicle control 1 hour before induction of IRI. After 18 hours, mice were euthanized, and kidneys were harvested. Before euthanasia, blood was drawn by retro-orbital bleed, and plasma creatinine was determined using a colorimetric assay according to the manufacturer's protocol (Sigma Aldrich).[25,26] All animal experiments were approved by the University of Virginia and Hospital for Sick Children Institutional Animal Care and Use Committees, and they adhered to the National Institutes of Health Guide for the Care and Use of Laboratory Animals.

Histologic Scores

Kidney sections (4 μm) were stained with hematoxylin and eosin, and images were obtained using a SPOT-RT Camera (software version 3.3; Diagnostic Instruments, Sterling Heights, MI) under 2× and 20× magnifications. For quantification of tubular injury score, sections were assessed by counting the percentage of tubules that displayed cell necrosis, loss of brush border, cast formation, and tubule dilation as follows: 1<10%, 2=10%–25%, 3=26%–50%;, 4=51%–75%, and 5>75%. Two to three fields from each outer medulla were evaluated and scored separately by two individuals masked to treatment categories.[26]

Flow Cytometry Analysis

After IRI, flow cytometry was used to quantify the infiltrating leukocyte subsets in the injured kidney.[25] In brief, kidneys were harvested, weighed, minced, and incubated with collagenase type IA (10 μg/ml; Sigma-Aldrich) in cold Dulbecco's PBS buffer with EDTA (2 mmol/L) for 15 minutes at 37°C. The digested kidney tissue suspension was teased through a 100-μm BD Falcon cell strainer (Fisher Scientific, Pittsburgh, PA) by the rubber end of a 1-ml syringe plunger, passed through a cotton column treated with 10% FCS, and centrifuged at 1200 rpm for 10 minutes. The cell pellet was washed with 1% BSA in PBS containing 0.1% sodium azide (Sigma-Aldrich). After blocking nonspecific Fc binding with anti-mouse CD16/32 antibody (2.4G2), fresh cell suspensions were incubated with fluorophore-tagged anti-mouse CD45 antibody (30-F11) to determine total leukocyte cell numbers. Anti-CD45 antibody-labeled samples were also labeled with different combinations of anti-mouse F4/80-APC antibody (BM8), anti-mouse GR-1-FITC antibody (Ly6G), and anti-mouse CD11b-PE antibody to identify macrophages (CD11b$^+$ F4/80^{low}) and neutrophils (CD11b$^+$ GR1$^+$).[25] 7-AAD (BD Biosciences, San Jose, CA) was added 15 minutes before analyzing the sample to separate live from dead cells.[25] Appropriate fluorochrome-conjugated, isotype-matched, irrelevant monoclonal antibodies were used as negative controls. Subsequent flow cytometry data acquisition was performed on BD FACS Calibur. Data were analyzed using FlowJo software 6.4 (Tree Star).[25] The number of GR-1$^+$CD11b$^+$CD45$^+$ neutrophils was normalized to kidney weight, indexed to the value for sham surgery kidneys, and log-transformed to generate a neutrophil infiltration score. Similarly, the number of CD11b$^+$ F4/80^{low} macrophages was normalized to kidney weight and indexed to the value of sham surgery kidneys to generate a macrophage infiltration score.

Slit2 Immunofluorescent Labeling

Immunofluorescent staining was performed on frozen sections of mouse kidney. Microwave antigen retrieval was carried out in citrate buffer for 20 minutes at medium-high setting (950 W maximum output, Panasonic NN-S758WC; Panasonic, Mississauga, ON, Canada) followed by 30 minutes of cooling at room temperature.[100] Sections were blocked and permeabilized in 2% donkey serum with 1% BSA and 0.1% Triton-X for 45 minutes and then incubated with anti-Slit2 antibody (8 μg/ml; Santa Cruz Biotech) at 4°C overnight. An Alexa 488-conjugated secondary antibody (1.5 μg/ml) in blocking reagent was incubated at room temperature for 2 hours. For some slides, autofluorescence of the surrounding renal cortex was captured in the red channel. For quantification, slides were treated with 0.05% sudan black (Sigma-Aldrich, St. Louis, MO) in 70% ethanol for 30 minutes at room temperature to reduce renal autofluorescence.[101] Kidney sections were mounted and visualized using a spinning disk DMIRE2 confocal microscope (Leica Microsystems, Toronto, ON, Canada) equipped with a Hamamatsu backthinned electron microscopy charge-coupled device camera. Images were acquired at 20× magnification and analyzed using Volocity software (Perkin-Elmer, Woodbridge, ON, Canada).

Murine Infection with *Listeria* Monocytogenes

Six- to eight-week-old C57BL/6J mice were purchased from Jackson Laboratory. N-mSlit2 (2 μg/mouse) or control vehicle was delivered by intravenous injection in the lateral tail vein. *L. monocytogenes* (5×10^4 CFU) in 200 μl PBS was injected intravenously 1 hour later.

Mice were euthanized at the indicated time points, and the livers were harvested. The left lobe of the liver was homogenized in sterile PBS for quantification of bacterial CFU from serial dilutions on brain heart infusion-agar plates. These experiments were approved by the Hospital for Sick Children Institutional Animal Care and Use Committee and adhered to the National Institutes of Health Guide for the Care and Use of Laboratory Animals.

Experimental Acute Pyelonephritis

As previously described, *E. coli* CFT073 was isolated from the blood and urine of a patient with acute pyelonephritis.[102] The functional virulence genes in *E. coli* CFT073 include *hly*1+, *pap*1+, *sfa*1+, and *pil*1+ as well as TcpC. *In vivo*, this strain is highly virulent in a mouse model of ascending urinary tract infection and exhibits *in vitro* cytotoxicity in cultured human renal proximal tubular epithelial cells.[103] The strains were grown at 37°C on solid Luria–Bertani agar and suspended in 10 ml PBS (pH 7.2) to generate the bacterial suspension used for infection (10^9 CFU/ml).

The ascending murine urinary tract infection experiments were performed as previously described.[37–39] Briefly, after isoflurane anesthesia, male BALB/c mice (8–12 weeks) were infected by intravesical inoculation (10^9 CFU/ml, 100 μl) through a soft polyethylene catheter (outer diameter=0.61 mm; Clay Adams, Parsippany, NY). The catheter was withdrawn, and the mice were allowed food and water *ad libitum*. One hour before inoculation, mice were intraperitoneally administered either N-mSlit2 (2 μg) or PBS vehicle. After designated time intervals, urine was collected into sterile tubes through gentle suprapubic pressure. After euthanasia, kidneys were retrieved using aseptic technique.

Bacterial numbers in urine and kidney homogenates were determined by viable counts. The organs were separately placed in a sterile plastic bag containing 5 ml PBS and homogenized in a Stomacher 80 homogenizer (Seward Medical, UAC House, London, United Kingdom). Homogenates were diluted in sterile PBS, and 0.1 ml each dilution were plated on tryptic soya agar. The number of colonies was scored after overnight culture at 37°C. Urine neutrophils were quantified on freshly isolated urine samples in a hemocytometer chamber as previously described.[38,39] The study was approved by the Animal Experiment Ethics Committee at the Lund district court in Sweden.

Statistical Analyses

All data are shown as mean ± SEM unless otherwise stated. Graphpad Prism (version 5.0; GraphPad Software, San Diego, CA) and SPSS statistical software (version 19.0; SPSS, Chicago, IL) were used to analyze the data. Data were analyzed using two-tailed t test or one-way ANOVA with posthoc analysis as appropriate. $P<0.05$ was used to indicate significance.

REFERENCES

1. Bagshaw SM: The long-term outcome after acute renal failure. *Curr Opin Crit Care* 12: 561–566, 2006
2. Brady HR, Singer GG: Acute renal failure. *Lancet* 346: 1533–1540, 1995
3. Korkeila M, Ruokonen E, Takala J: Costs of care, long-term prognosis and quality of life in patients requiring renal replacement therapy during intensive care. *Intensive Care Med* 26: 1824–1831, 2000
4. Thadhani R, Pascual M, Bonventre JV: Acute renal failure. *N Engl J Med* 334: 1448–1460, 1996
5. Jo SK, Rosner MH, Okusa MD: Pharmacologic treatment of acute kidney injury: Why drugs haven't worked and what is on the horizon. *Clin J Am Soc Nephrol* 2: 356–365, 2007
6. Day Y-J, Huang L, Ye H, Linden J, Okusa MD: Renal ischemia-reperfusion injury and adenosine 2A receptor-mediated tissue protection: Role of macrophages. *Am J Physiol Renal Physiol* 288: F722–F731, 2005
7. Loverre A, Capobianco C, Stallone G, Infante B, Schena A, Ditonno P, Palazzo S, Battaglia M, Crovace A, Castellano G, Ranieri E, Schena FP, Gesualdo L, Grandaliano G: Ischemia-reperfusion injury-induced abnormal dendritic cell traffic in the transplanted kidney with delayed graft function. *Kidney Int* 72: 994–1003, 2007
8. Okusa MD: The inflammatory cascade in acute ischemic renal failure. *Nephron* 90: 133–138, 2002
9. Rabb H, Daniels F, O'Donnell M, Haq M, Saba SR, Keane W, Tang WW: Pathophysiological role of T lymphocytes in renal ischemia-reperfusion injury in mice. *Am J Physiol Renal Physiol* 279: F525–F531, 2000
10. Fiorina P, Ansari MJ, Jurewicz M, Barry M, Ricchiuti V, Smith RN, Shea S, Means TK, Auchincloss HJ Jr, Luster AD, Sayegh MH, Abdi R: Role of CXC chemokine receptor 3 pathway in renal ischemic injury. *J Am Soc Nephrol* 17: 716–723, 2006
11. Friedewald JJ, Rabb H: Inflammatory cells in ischemic acute renal failure. *Kidney Int* 66: 486–491, 2004
12. Furuichi K, Wada T, Iwata Y, Kitagawa K, Kobayashi K, Hashimoto H, Ishiwata Y, Asano M, Wang H, Matsushima K, Takeya M, Kuziel WA, Mukaida N, Yokoyama H: CCR2 signaling contributes to ischemia-reperfusion injury in kidney. *J Am Soc Nephrol* 14: 2503–2515, 2003
13. Kelly KJ, Williams WW Jr, Colvin RB, Bonventre JV: Antibody to intercellular adhesion molecule 1 protects the kidney against ischemic injury. *Proc Natl Acad Sci U S A* 91: 812–816, 1994
14. Singbartl K, Green SA, Ley K: Blocking P-selectin protects from ischemia/reperfusion-induced acute renal failure. *FASEB J* 14: 48–54, 2000
15. Salmela K, Wramner L, Ekberg H, Hauser I, Bentdal O, Lins LE, Isoniemi H, Bäckman L, Persson N, Neumayer HH, Jørgensen PF, Spieker C, Hendry B, Nicholls A, Kirste G, Hasche G: A randomized

multicenter trial of the anti-ICAM-1 monoclonal antibody (enlimomab) for the prevention of acute rejection and delayed onset of graft function in cadaveric renal transplantation: A report of the European Anti-ICAM-1 Renal Transplant Study Group. *Transplantation* 67: 729–736, 1999

16. Brose K, Bland KS, Wang KH, Arnott D, Henzel W, Goodman CS, Tessier-Lavigne M, Kidd T: Slit proteins bind Robo receptors and have an evolutionarily conserved role in repulsive axon guidance. *Cell* 96: 795–806, 1999

17. Kidd T, Brose K, Mitchell KJ, Fetter RD, Tessier-Lavigne M, Goodman CS, Tear G: Roundabout controls axon crossing of the CNS midline and defines a novel subfamily of evolutionarily conserved guidance receptors. *Cell* 92: 205–215, 1998

18. Hohenester E: Structural insight into Slit-Robo signalling. *Biochem Soc Trans* 36: 251–256, 2008

19. Wong K, Park H-T, Wu JY, Rao Y: Slit proteins: Molecular guidance cues for cells ranging from neurons to leukocytes. *Curr Opin Genet Dev* 12: 583–591, 2002

20. Guan H, Zu G, Xie Y, Tang H, Johnson M, Xu X, Kevil C, Xiong WC, Elmets C, Rao Y, Wu JY, Xu H: Neuronal repellent Slit2 inhibits dendritic cell migration and the development of immune responses. *J Immunol* 171: 6519–6526, 2003

21. Prasad A, Qamri Z, Wu J, Ganju RK: Slit-2/Robo-1 modulates the CXCL12/CXCR4-induced chemotaxis of T cells. *J Leukoc Biol* 82: 465–476, 2007

22. Tole S, Mukovozov IM, Huang YW, Magalhaes MA, Yan M, Crow MR, Liu GY, Sun CX, Durocher Y, Glogauer M, Robinson LA: The axonal repellent, Slit2, inhibits directional migration of circulating neutrophils. *J Leukoc Biol* 86: 1403–1415, 2009

23. Wu JY, Feng L, Park H-T, Havlioglu N, Wen L, Tang H, Bacon KB, Jiang Zh, Zhang Xc, Rao Y: The neuronal repellent Slit inhibits leukocyte chemotaxis induced by chemotactic factors. *Nature* 410: 948–952, 2001

24. Li L, Huang L, Sung SS, Lobo PI, Brown MG, Gregg RK, Engelhard VH, Okusa MD: NKT cell activation mediates neutrophil IFN-gamma production and renal ischemia-reperfusion injury. *J Immunol* 178: 5899–5911, 2007

25. Li L, Huang L, Sung SS, Vergis AL, Rosin DL, Rose CE Jr, Lobo PI, Okusa MD: The chemokine receptors CCR2 and CX3CR1 mediate monocyte/macrophage trafficking in kidney ischemia-reperfusion injury. *Kidney Int* 74: 1526–1537, 2008

26. Li L, Huang L, Vergis AL, Ye H, Bajwa A, Narayan V, Strieter RM, Rosin DL, Okusa MD: IL-17 produced by neutrophils regulates IFN-gamma-mediated neutrophil migration in mouse kidney ischemia-reperfusion injury. *J Clin Invest* 120: 331–342, 2010

27. Donnahoo KK, Meng X, Ayala A, Cain MP, Harken AH, Meldrum DR: Early kidney TNF-alpha expression mediates neutrophil infiltration and injury after renal ischemia-reperfusion. *Am J Physiol* 277: R922–R929, 1999

28. Wu W, Wong K, Chen J, Jiang Z, Dupuis S, Wu JY, Rao Y: Directional guidance of neuronal migration in the olfactory system by the protein Slit. *Nature* 400: 331–336, 1999

29. Dickinson RE, Myers M, Duncan WC: Novel regulated expression of the SLIT/ROBO pathway in the ovary: Possible role during luteolysis in women. *Endocrinology* 149: 5024–5034, 2008

30. Pieters R, Huismans DR, Leyva A, Veerman AJ: Adaptation of the rapid automated tetrazolium dye based (MTT) assay for chemosensitivity testing in childhood leukemia. *Cancer Lett* 41: 323–332, 1988

31. Zarbock A, Ley K: Neutrophil adhesion and activation under flow. *Microcirculation* 16: 31–42, 2009

32. Adamson P, Etienne S, Couraud PO, Calder V, Greenwood J: Lymphocyte migration through brain endothelial cell monolayers involves signaling through endothelial ICAM-1 via a rho-dependent pathway. *J Immunol* 162: 2964–2973, 1999

33. Bayat B, Werth S, Sachs UJ, Newman DK, Newman PJ, Santoso S: Neutrophil transmigration mediated by the neutrophil-specific antigen CD177 is influenced by the endothelial S536N dimorphism of platelet endothelial cell adhesion molecule-1. *J Immunol* 184: 3889–3896, 2010

34. van Wetering S, van den Berk N, van Buul JD, Mul FPJ, Lommerse I, Mous R, ten Klooster JP, Zwaginga JJ, Hordijk PL: VCAM-1-mediated Rac signaling controls endothelial cell-cell contacts and leukocyte transmigration. *Am J Physiol Cell Physiol* 285: C343–C352, 2003

35. Caron E, Hall A: Identification of two distinct mechanisms of phagocytosis controlled by different Rho GTPases. *Science* 282: 1717–1721, 1998

36. Conlan JW, North RJ: Neutrophils are essential for early anti-Listeria defense in the liver, but not in the spleen or peritoneal cavity, as revealed by a granulocyte-depleting monoclonal antibody. *J Exp Med* 179: 259–268, 1994

37. Connell I, Agace W, Klemm P, Schembri M, Mărild S, Svanborg C: Type 1 fimbrial expression enhances Escherichia coli virulence for the urinary tract. *Proc Natl Acad Sci U S A* 93: 9827–9832, 1996

38. Svensson M, Irjala H, Svanborg C, Godaly G: Effects of epithelial and neutrophil CXCR2 on innate immunity and resistance to kidney infection. *Kidney Int* 74: 81–90, 2008

39. Godaly G, Hang L, Frendéus B, Svanborg C: Transepithelial neutrophil migration is CXCR1 dependent in vitro and is defective in IL-8 receptor knockout mice. *J Immunol* 165: 5287–5294, 2000

40. Haraoka M, Hang L, Frendéus B, Godaly G, Burdick M, Strieter R, Svanborg C: Neutrophil recruitment and resistance to urinary tract infection. *J Infect Dis* 180: 1220–1229, 1999

41. Xue JL, Daniels F, Star RA, Kimmel PL, Eggers PW, Molitoris BA, Himmelfarb J, Collins AJ: Incidence and mortality of acute renal failure in Medicare beneficiaries, 1992 to 2001. *J Am Soc Nephrol* 17: 1135–1142, 2006

42. Devarajan P: Update on mechanisms of ischemic acute kidney injury. *J Am Soc Nephrol* 17: 1503–1520, 2006

43. Star RA: Treatment of acute renal failure. *Kidney Int* 54: 1817–1831, 1998

44. Bolisetty S, Agarwal A: Neutrophils in acute kidney injury: Not neutral any more. *Kidney Int* 75: 674–676, 2009

45. Awad AS, Rouse M, Huang L, Vergis AL, Reutershan J, Cathro HP, Linden J, Okusa MD: Compartmentalization of neutrophils in the kidney and lung following acute ischemic kidney injury. *Kidney Int* 75: 689–698, 2009

46. Kato N, Yuzawa Y, Kosugi T, Hobo A, Sato W, Miwa Y, Sakamoto K, Matsuo S, Kadomatsu K: The E-selectin ligand basigin/CD147 is responsible for neutrophil recruitment in renal ischemia/reperfusion. *J Am Soc Nephrol* 20: 1565–1576, 2009

47. Nemoto T, Burne MJ, Daniels F, O'Donnell MP, Crosson J, Berens K, Issekutz A, Kasiske BL, Keane WF, Rabb H: Small molecule selectin ligand inhibition improves outcome in ischemic acute renal failure. *Kidney Int* 60: 2205–2214, 2001

48. Kidd T, Bland KS, Goodman CS: Slit is the midline repellent for the robo receptor in Drosophila. *Cell* 96: 785–794, 1999

49. Millán J, Ridley AJ: Rho GTPases and leucocyte-induced endothelial remodelling. *Biochem J* 385: 329–337, 2005

50. Hall A: Rho GTPases and the actin cytoskeleton. *Science* 279: 509–514, 1998

51. Nobes CD, Hall A: Rho, rac, and cdc42 GTPases regulate the assembly of multimolecular focal complexes associated with actin stress fibers, lamellipodia, and filopodia. *Cell* 81: 53–62, 1995

52. Raftopoulou M, Hall A: Cell migration: Rho GTPases lead the way. *Dev Biol* 265: 23–32, 2004

53. Wójciak-Stothard B, Williams L, Ridley AJ: Monocyte adhesion and spreading on human endothelial cells is dependent on Rho-regulated receptor clustering. *J Cell Biol* 145: 1293–1307, 1999

54. Weber KS, Klickstein LB, Weber PC, Weber C: Chemokine-induced monocyte transmigration requires cdc42-mediated cytoskeletal changes. *Eur J Immunol* 28: 2245–2251, 1998

55. Worthylake RA, Lemoine S, Watson JM, Burridge K: RhoA is required for monocyte tail retraction during transendothelial migration. *J Cell Biol* 154: 147–160, 2001

56. Filippi MD, Szczur K, Harris CE, Berclaz PY: Rho GTPase Rac1 is critical for neutrophil migration into the lung. *Blood* 109: 1257–1264, 2007

57. Yonemura S, Matsui T, Tsukita S, Tsukita S: Rho-dependent and -independent activation mechanisms of ezrin/radixin/moesin proteins: An essential role for polyphosphoinositides in vivo. *J Cell Sci* 115: 2569–2580, 2002

58. Nijhara R, van Hennik PB, Gignac ML, Kruhlak MJ, Hordijk PL, Delon J, Shaw S: Rac1 mediates collapse of microvilli on chemokine-activated T lymphocytes. *J Immunol* 173: 4985–4993, 2004

59. Kanellis J, Garcia GE, Li P, Parra G, Wilson CB, Rao Y, Han S, Smith CW, Johnson RJ, Wu JY, Feng L: Modulation of inflammation by slit protein in vivo in experimental crescentic glomerulonephritis. *Am J Pathol* 165: 341–352, 2004

60. Glogauer M, Marchal CC, Zhu F, Worku A, Clausen BE, Foerster I, Marks P, Downey GP, Dinauer M, Kwiatkowski DJ: Rac1 deletion in mouse neutrophils has selective effects on neutrophil functions. *J Immunol* 170: 5652–5657, 2003

61. Gu Y, Filippi MD, Cancelas JA, Siefring JE, Williams EP, Jasti AC, Harris CE, Lee AW, Prabhakar R, Atkinson SJ, Kwiatkowski DJ, Williams DA: Hematopoietic cell regulation by Rac1 and Rac2 guanosine triphosphatases. *Science* 302: 445–449, 2003

62. Pai SY, Kim C, Williams DA: Rac GTPases in human diseases. *Dis Markers* 29: 177–187, 2010

63. Diebold BA, Fowler B, Lu J, Dinauer MC, Bokoch GM: Antagonistic cross-talk between Rac and Cdc42 GTPases regulates generation of reactive oxygen species. *J Biol Chem* 279: 28136–28142, 2004

64. Srinivasan S, Wang F, Glavas S, Ott A, Hofmann F, Aktories K, Kalman D, Bourne HR: Rac and Cdc42 play distinct roles in regulating PI(3,4,5)P3 and polarity during neutrophil chemotaxis. *J Cell Biol* 160: 375–385, 2003

65. Hampton MB, Kettle AJ, Winterbourn CC: Involvement of superoxide and myeloperoxidase in oxygen-dependent killing of Staphylococcus aureus by neutrophils. *Infect Immun* 64: 3512–3517, 1996

66. Yeh MC, Mukaro V, Hii CS, Ferrante A: Regulation of neutrophil-mediated killing of Staphylococcus aureus and chemotaxis by c-jun NH2 terminal kinase. *J Leukoc Biol* 87: 925–932, 2010

67. Dinauer MC, Deck MB, Unanue ER: Mice lacking reduced nicotinamide adenine dinucleotide phosphate oxidase activity show increased susceptibility to early infection with Listeria monocytogenes. *J Immunol* 158: 5581–5583, 1997

68. LaCourse R, Ryan L, North RJ: Expression of NADPH oxidase-dependent resistance to listeriosis in mice occurs during the first 6 to 12 hours of liver infection. *Infect Immun* 70: 7179–7181, 2002

69. Patel S, Huang YW, Reheman A, Pluthero FG, Chaturvedi S, Mukovozov IM, Tole S, Liu GY, Li L, Durocher Y, Ni H, Kahr WH, Robinson LA: The cell motility modulator Slit2 is a potent inhibitor of platelet function. *Circulation* 126: 1385–1395, 2012

70. Weyrich AS, Elstad MR, McEver RP, McIntyre TM, Moore KL, Morrissey JH, Prescott SM, Zimmerman GA: Activated platelets signal chemokine synthesis by human monocytes. *J Clin Invest* 97: 1525–1534, 1996

71. Deuel TF, Senior RM, Chang D, Griffin GL, Heinrikson RL, Kaiser ET: Platelet factor 4 is chemotactic for neutrophils and monocytes. *Proc Natl Acad Sci U S A* 78: 4584–4587, 1981

72. von Hundelshausen P, Weber KS, Huo Y, Proudfoot AE, Nelson PJ, Ley K, Weber C: RANTES deposition by platelets triggers monocyte arrest on inflamed and atherosclerotic endothelium. *Circulation* 103: 1772–1777, 2001

73. Li L, Okusa MD: Blocking the immune response in ischemic acute kidney injury: The role of adenosine 2A agonists. *Nat Clin Pract Nephrol* 2: 432–444, 2006

74. Sharfuddin AA, Molitoris BA: Pathophysiology of ischemic acute kidney injury. *Nat Rev Nephrol* 7: 189–200, 2011

75. Singbartl K, Forlow SB, Ley K: Platelet, but not endothelial, P-selectin is critical for neutrophil-mediated acute postischemic renal failure. *FASEB J* 15: 2337–2344, 2001

76. Jo SK, Sung SA, Cho WY, Go KJ, Kim HK: Macrophages contribute to the initiation of ischaemic acute renal failure in rats. *Nephrol Dial Tranplant* 21: 1231–1239, 2006

77. Kelly KJ, Williams WW Jr, Colvin RB, Meehan SM, Springer TA, Gutierrez-Ramos JC, Bonventre JV: Intercellular adhesion molecule-1-deficient mice are protected against ischemic renal injury. *J Clin Invest* 97: 1056–1063, 1996

78. Allport JR, Ding HT, Ager A, Steeber DA, Tedder TF, Luscinskas FW: L-selectin shedding does not regulate human neutrophil attachment, rolling, or transmigration across human vascular endothelium in vitro. *J Immunol* 158: 4365–4372, 1997

79. Robinson LA, Tu L, Steeber DA, Preis O, Platt JL, Tedder TF: The role of adhesion molecules in human leukocyte attachment to porcine vascular endothelium: Implications for xenotransplantation. *J Immunol* 161: 6931–6938, 1998

80. Brady HR, Spertini O, Jimenez W, Brenner BM, Marsden PA, Tedder TF: Neutrophils, monocytes, and lymphocytes bind to cytokine-activated kidney glomerular endothelial cells through L-selectin (LAM-1) in vitro. *J Immunol* 149: 2437–2444, 1992

81. Foreman KE, Vaporciyan AA, Bonish BK, Jones ML, Johnson KJ, Glovsky MM, Eddy SM, Ward PA: C5a-induced expression of P-selectin in endothelial cells. *J Clin Invest* 94: 1147–1155, 1994

82. Arnould T, Michiels C, Remacle J: Hypoxic human umbilical vein endothelial cells induce activation of adherent polymorphonuclear leukocytes. *Blood* 83: 3705–3716, 1994

83. Canty TG Jr, Boyle EM Jr, Farr A, Morgan EN, Verrier ED, Pohlman TH: Oxidative stress induces NF-kappaB nuclear translocation without degradation of IkappaBalpha. *Circulation* 100[Suppl]: II361–II364, 1999

84. Farivar AS, Mackinnon-Patterson BC, Barnes AD, McCourtie AS, Mulligan MS: Cyclosporine modulates the response to hypoxia-reoxygenation in pulmonary artery endothelial cells. *Ann Thorac Surg* 79: 1010–1016, 2005

85. Koo DD, Welsh KI, West NE, Channon KM, Penington AJ, Roake JA, Morris PJ, Fuggle SV: Endothelial cell protection against ischemia/reperfusion injury by lecithinized superoxide dismutase. *Kidney Int* 60: 786–796, 2001

86. Ichikawa H, Flores S, Kvietys PR, Wolf RE, Yoshikawa T, Granger DN, Aw TY: Molecular mechanisms of anoxia/reoxygenation-induced neutrophil adherence to cultured endothelial cells. *Circ Res* 81: 922–931, 1997

87. Fong AM, Robinson LA, Steeber DA, Tedder TF, Yoshie O, Imai T, Patel DD: Fractalkine and CX3CR1 mediate a novel mechanism of leukocyte capture, firm adhesion, and activation under physiologic flow. *J Exp Med* 188: 1413–1419, 1998

88. Kuckleburg CJ, Tilkens SB, Santoso S, Newman PJ: Proteinase 3 contributes to transendothelial migration of NB1-positive neutrophils. *J Immunol* 188: 2419–2426, 2012

89. Chen C, Khismatullin DB: Synergistic effect of histamine and TNF-α on monocyte adhesion to vascular endothelial cells. *Inflammation* 36: 309–319, 2013

90. Brevig T, Krühne U, Kahn RA, Ahl T, Beyer M, Pedersen LH: Hydrodynamic guiding for addressing subsets of immobilized cells and molecules in microfluidic systems. *BMC Biotechnol* 3: 10, 2003

91. Schaff U, Mattila PE, Simon SI, Walcheck B: Neutrophil adhesion to E-selectin under shear promotes the redistribution and co-clustering of ADAM17 and its proteolytic substrate L-selectin. *J Leukoc Biol* 83: 99–105, 2008

92. Ting HJ, Stice JP, Schaff UY, Hui DY, Rutledge JC, Knowlton AA, Passerini AG, Simon SI: Triglyceride-rich lipoproteins prime aortic endothelium for an enhanced inflammatory response to tumor necrosis factor-alpha. *Circ Res* 100: 381–390, 2007

93. Srigunapalan S, Lam C, Wheeler AR, Simmons CA: A microfluidic membrane device to mimic critical components of the vascular microenvironment. *Biomicrofluidics* 5: 13409, 2011

94. Ahrens I, Ellwanger C, Smith BK, Bassler N, Chen YC, Neudorfer I, Ludwig A, Bode C, Peter K: Selenium supplementation induces metalloproteinase-dependent L-selectin shedding from monocytes. *J Leukoc Biol* 83: 1388–1395, 2008

95. Simon SI, Hu Y, Vestweber D, Smith CW: Neutrophil tethering on E-selectin activates beta 2 integrin binding to ICAM-1 through a mitogen-activated protein kinase signal transduction pathway. *J Immunol* 164: 4348–4358, 2000

96. Jones DA, Smith CW, Picker LJ, McIntire LV: Neutrophil adhesion to 24-hour IL-1-stimulated endothelial cells under flow conditions. *J Immunol* 157: 858–863, 1996

97. Smith WB, Gamble JR, Clark-Lewis I, Vadas MA: Interleukin-8 induces neutrophil transendothelial migration. *Immunology* 72: 65–72, 1991

98. Takahashi M, Masuyama J, Ikeda U, Kitagawa S, Kasahara T, Saito M, Kano S, Shimada K: Effects of endogenous endothelial interleukin-8 on neutrophil migration across an endothelial monolayer. *Cardiovasc Res* 29: 670–675, 1995

99. Yan M, Di Ciano-Oliveira C, Grinstein S, Trimble WS: Coronin function is required for chemotaxis and phagocytosis in human neutrophils. *J Immunol* 178: 5769–5778, 2007

100. Waters AM, Wu MYJ, Onay T, Scutaru J, Liu J, Lobe CG, Quaggin SE, Piscione TD: Ectopic notch activation in developing podocytes causes glomerulosclerosis. *J Am Soc Nephrol* 19: 1139–1157, 2008

101. Sun Y, Yu H, Zheng D, Cao Q, Wang Y, Harris D, Wang Y: Sudan black B reduces autofluorescence in murine renal tissue. *Arch Pathol Lab Med* 135: 1335–1342, 2011

102. Kao JS, Stucker DM, Warren JW, Mobley HL: Pathogenicity island sequences of pyelonephritogenic Escherichia coli CFT073 are associated with virulent uropathogenic strains. *Infect Immun* 65: 2812–2820, 1997

103. Mobley HL, Green DM, Trifillis AL, Johnson DE, Chippendale GR, Lockatell CV, Jones BD, Warren JW: Pyelonephritogenic Escherichia coli and killing of cultured human renal proximal tubular epithelial cells: Role of hemolysin in some strains. *Infect Immun* 58: 1281–1289, 1990